Journal of Photonics for Energy

PhotonicsforEnergy.SPIEDigitalLibrary.org

Efficiency of broadband terahertz rectennas based on self-switching nanodiodes

Edgar Briones
Irving E. Cortes-Mestizo
Joel Briones
Ravindranath Droopad
Leticia I. Espinosa-Vega
Heber Vilchis
Victor H. Mendez-Garcia

SPIE.

Edgar Briones, Irving E. Cortes-Mestizo, Joel Briones, Ravindranath Droopad, Leticia I. Espinosa-Vega, Heber Vilchis, Victor H. Mendez-Garcia, "Efficiency of broadband terahertz rectennas based on self-switching nanodiodes," *J. Photon. Energy* **7**(2), 025001 (2017), doi: 10.1117/1.JPE.7.025001.

Efficiency of broadband terahertz rectennas based on self-switching nanodiodes

Edgar Briones,[a] Irving E. Cortes-Mestizo,[b] Joel Briones,[a] Ravindranath Droopad,[c] Leticia I. Espinosa-Vega,[b] Heber Vilchis,[d] and Victor H. Mendez-Garcia[b,*]

[a]ITESO Jesuit University of Guadalajara, Department of Mathematics and Physics, Tlaquepaque, Mexico

[b]Universidad Autónoma de San Luis Potosí, CIACyT, San Luis Potosí, Mexico

[c]Texas State University, Ingram School of Engineering, San Marcos, Texas, United States

[d]Universidad de Ciencias y Artes de Chiapas, Centro de Investigación y Desarrollo Tecnológico en Energías Renovables, Tuxtla Gutiérrez, Mexico

Abstract. The authors investigate the efficiency of a series of broadband rectennas designed to harvest the free-propagating electromagnetic energy at terahertz frequencies. We analyze by simulations the case of self-complementary square- and Archimedean-spiral antennas coupled to L-shaped self-switching diodes (L-SSDs). First, the geometry (i.e., the width and length of the channel) of the L-SSD was optimized to obtain a remarkable diode-like I–V response. Subsequently, the optimized L-SSD geometry was coupled to both types of spiral antennas and their characteristic impedance was studied. Finally, the energy conversion efficiency was evaluated for both rectenna architectures. © *2017 Society of Photo-Optical Instrumentation Engineers (SPIE)* [DOI: 10.1117/1.JPE.7.025001]

Keywords: terahertz; self-switching diodes; spirals antennas; energy harvesting; impedance matching.

Paper 16135 received Dec. 16, 2016; accepted for publication Mar. 31, 2017; published online Apr. 27, 2017.

1 Introduction

Infrared rectennas have attracted a great deal of research interest in recent years due to their ability to convert optical energy into direct current (DC) power.[1] These devices are composed of an antenna that collects the radiation and converts it into an alternating current (AC),[2] and a high-speed diode that rectifies the AC.[3] Since the conversion efficiency of the rectennas is high,[4,5] they show a great potential in the design of photovoltaic devices that can operate at infrared wavelengths. For instance, they can be used to harvest the radiation reemitted by the Earth,[3,6,7] which covers the spectral range from 7 to 20 μm,[8] and the radiation emitted by some other artificial thermal sources, such as engines, furnaces, etc., as they emit radiation at longer wavelengths (submillimeter wavelengths or terahertz frequencies).

Rectennas have been employed as an efficient mechanism to convert the energy of microwaves into DC power,[9] but their use at shorter wavelengths, or equivalent higher frequencies, has been limited by the lack of efficient rectifiers at this radiation range. Most of the high-frequency rectifiers are nanometer-sized diodes based on vertical tunnel barriers,[10,11] which are able to operate at visible frequencies.[12] However, they exhibit a high-resistance and poor-asymmetric current–voltage characteristics due to their nanometer size and the materials employed for their fabrication. Both of these factors drastically drop the efficiency of the rectennas.[13] In this regard, diodes based on rectifying mechanisms are currently being investigated with the purpose to circumvent these constraints,[14] e.g., metal–semiconductor–metal heterojunction diodes have

*Address all correspondence to: Victor H. Mendez-Garcia, E-mail: victor.mendez@uaslp.mx

1947-7988/2017/$25.00 © 2017 SPIE

reduced the zero-bias resistance while keeping a high-current density, and as a result, the antenna rectifier matching is improved, however, its manufacture is complex.[15]

A concept of an electronic device employed for efficient rectification at high frequencies with a simple planar architecture is the so-called self-switching diode (SSD). An SSD consists of a nanometer-sized semiconductor channel created between two L-shaped insulator grooves,[16] in which the electronic transport along the channel is allowed along one direction while it is suppressed in the other, leading to a remarkably diode-like behavior. This effect is due to electric field effects induced by the near surface charge redistribution between the lateral surface states at the groove walls and the depletion region extended inside the channel.[16,17] Several investigations have been conducted to improve diode-like characteristics of channels and their response at high frequencies, leading to the development of diodes with an excellent performance at gigahertz and even terahertz frequencies.[17–20] These properties make the SSDs promising candidates for the development of new types of rectennas that could operate in the terahertz band (or the submillimeter range) where there is a lack of compact, low-cost, and efficient technologies.

In recent years, SSDs have been incorporated into dipole, bowtie,[18] and spiral[20] antennas to develop zero-bias terahertz rectenna detectors. Such detectors have been successfully employed to sense radiation at 1.5 THz. Later, their use was extended to energy harvesting applications to convert the radiation emitted by a black-body at 973 K into DC power with an efficiency of 0.02%.[21] In this study, we evaluate the efficiency of terahertz rectennas employing Archimedean- and square-spiral antennas and we discuss their suitability and scope for energy harvesting applications when they are coupled to the SSD nanochannels, which are ideal for harvesting applications due to their absorption broadband. The spirals were coupled to SSD nanochannels manufactured in two-dimensional (2-D) electron gas (2DEG) InAlAs/InGaAs heterostructures. These structures are usually grown by molecular beam epitaxy. First, InAlAs buffer layers are grown on $In_{0.75}Ga_{0.25}As/InP$ substrates. Then, an 80-nm thick InGaAs layer is deposited followed by a 50-nm thick InAlAs film. The structure is capped with an InGaAs layer with 10 nm of thickness. All the layers are undoped and lattice matched to the substrate. The 2DEG is created at the interface InAlAs/InGaAs heterostructure by inserting a δ-doping layer above 20 nm of the InGaAs film within the InAlAs layer.[22] The geometry and dimensions of the SSD devices were chosen to enhance the conversion efficiency of the rectennas and the optical and transport properties were analyzed through numerical simulations.

2 Self-switching Diodes for Square Law-Rectification

The L-shaped channel studied in this work is shown in Fig. 1(a). This nanodiode is the most explored channel's geometry presenting the self-switching behavior and it can be assumed as a 2-D field-effect transistor with the gate to drain in short-circuit,[16,20] while the trenches of the channels act as double lateral gates. The analysis was performed for the InAlAs/InGaAs heterostructure described in the introduction considering the geometry shown in Fig. 1(a) by using a commercially available technology computer-assisted design software, in which a simplified 2-D model was developed with the top-view approximation similar to those reported for 2DEG-based InGaAs SSD and SOI.[19,23,24] The 2-D approach has been proved by other authors using Montecarlo simulations.[19] The model is applied to the 2DEG plane at room temperature where the mobility and background doping are equal to 12,000 cm^2/vs and 1×10^{17} cm^{-3}, respectively.[16,19] Additionally, the energy balance model was used to find the carrier distribution in the 2DEG plane, as well as its dependence on the applied voltage. To account for the effects in the surface-states, a charge density of 0.4×10^{12} cm^{-2} on the lateral surface trenches, i.e., at the interface between the semiconductors and vacuum, was assumed.[19] The contact resistivity used in the electrodes was set to 1×10^{-8} $\Omega \cdot cm^2$, a typical value for InGaAs devices.[25]

In Fig. 1(b) the carrier distribution of the SSD without any external applied voltage is presented. Under this condition, the electron density decreases along the channel and also progressively decreases toward the groove walls originated by the electron filling of acceptor-like states on the surface of the groove walls. Figures 1(c) and 1(d) show the charge distribution of the SSD channels under reverse and a forward bias, respectively. As observed, the reverse (forward) current is suppressed (enhanced) due to a self-induced field-effect that reduces (increases) the carrier density along the channel, leading to a clear diode-like behavior.

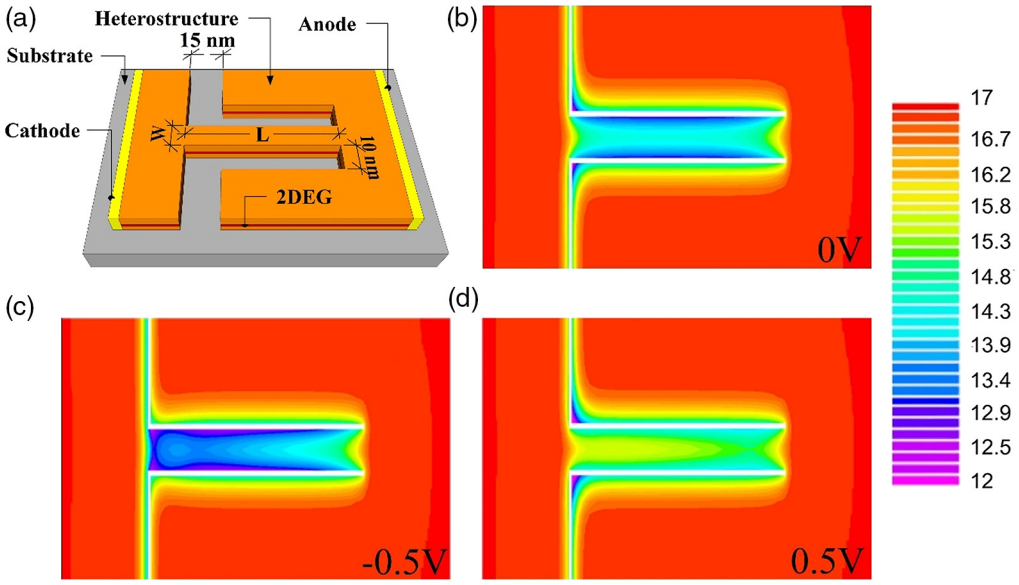

Fig. 1 (a) Schematic 3-D representation of an L-SSDs. The calculated electron density distribution (cm^{-3}, in logarithmic scale) of the L-SSDs is exhibited at (b) zero bias, (c) reverse bias, and (d) forward bias.

For harvesting applications, the diode-like behavior of these SSDs should be optimized first. The transport properties depend on the geometrical parameters, such as the width (W) and length (L) of the nanochannel. Thus, the optimization can be performed by adjusting the size of these parameters. The parameter that mostly affects the diode-like behavior of these structures and indeed the voltage threshold is W.[18,19] In this direction, we have performed a series of transport simulations in which the width of a channel was varied from 60 to 80 nm while the rest of their geometrical parameters were kept fixed: $L = 1$ μm and the width of the trenches was set at 10 and 15 nm as shown in Fig. 1(a).

The obtained DC current–voltage characteristics are shown in Fig. 2(a). For SSDs, it is desirable to get a clear diode-like behavior, i.e., the reverse (forward) current is suppressed (enhanced) due to a self-induced field-effect that decreases (increases) the carrier density along the channel. Therefore, according to Fig. 2(a) the optimal channel width value is reached at $W = 70$ nm (for $L = 1$ μm). It is worth noticing that the structures with $W = 70$ nm exhibit a low-voltage threshold ~40 mV (value found with a piecewise linear model), a condition that is desired in devices for energy harvesting applications. However, if W is reduced to 60 nm, the threshold is increased up to 200 mV, making it unsuitable for energy harvesting applications. For instance, if W is raised to 80 nm, the threshold decreases to ~0 mV, nevertheless, the current–voltage characteristics exhibit a poor diode-like behavior. The carrier density is strongly reduced inside the narrow channels because the depletion zone extends completely within the channels. As a consequence, trade-offs between the diode-like behavior and the voltage threshold take place, and these kinds of effects have been previously reported.[16]

Once the optimal channel width was found, a complementary study was performed to optimize the channels' length L, which is a parameter that also affects the current–voltage diode-like characteristics. L was varied from 200 nm to 1.5 μm whereas W was kept fixed at 70 nm; and the width of the trenches was set once again as shown in Fig. 1(a). The results are plotted in Fig. 2(b). Channels whose lengths are shorter than 1 μm present a poor diode-like behavior, whereas for lengths L larger than 1 μm, the diode-like behavior of the channels is improved. Since the SSD is essentially a field-effect transistor but with a short-circuited gate to drain, this effect can be considered as a short-channel effect. It is important to mention that the speed of operation of the SSDs depends on L, for instance, high-switching action will occur at a short channel. This is due to the short-travel path of electrons between the device electrodes and the lower-channel resistance (hence, a smaller resistance-capacitance time constant).[19]

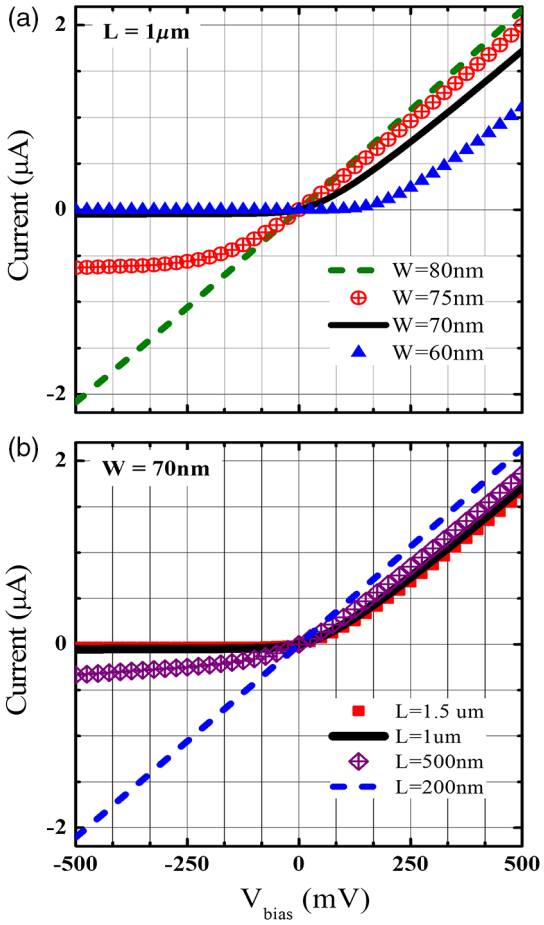

Fig. 2 Current–voltage response of a self-switching diode based on an InGaAs/InAlAs heterostructure as a function of (a) the channel width and (b) the channel length.

The DC current–voltage curves of the optimized channels were employed to study their rectifying properties. In the regime of low-AC voltages, the channels act as square-law rectifiers[26] and devices that generate a DC voltage whose amplitude is given by

$$V_{\mathrm{DC}} = -\frac{1}{4}\frac{I''(V_{\mathrm{bias}})}{I'(V_{\mathrm{bias}})}V_{\mathrm{AC}}^2 = -\frac{1}{4}\cdot\gamma\cdot V_{\mathrm{AC}}^2, \tag{1}$$

where V_{AC} is the amplitude of the AC voltage supplied to the channels and $I''(V_{\mathrm{bias}})/I'(V_{\mathrm{bias}})$ denotes the ratio of the second derivative to the first derivative of the DC current–voltage curve, commonly referred to as the rectifier sensitivity, γ. The sensitivity of the channels is a parameter that indicates how efficient the devices are; the higher the sensitivity, the higher the DC output.

Figure 3(a) shows the current–voltage curve of the optimized L-shape channel, $W = 70$ nm and $L = 1$ μm, where a near zero-threshold voltage can be appreciated. By employing the first derivative, the resistance R_0 can be obtained through the relationship $I'(V_{\mathrm{bias}})^{-1}$. Figures 3(b) and 3(c) show R_0 and γ as a function of the applied bias, respectively. At zero bias, R_0 is $\sim$0.8 MΩ and γ is $\sim$20 V^{-1}. At zero bias, it has been reported that the best metal–insulator–metal–tunnel barriers such as the polysilicon–SiO_2–polysilicon thin films exhibit sensitivity close to 2.5 V^{-1}, while for Cu/CuO/Au MIM ultra-thin barriers γ is close to 4 V^{-1}.[27,28] By employing SSDs as rectifiers, the sensitivity could be increased by a factor of five to eight. In this regard, it is worth mentioning that the performance of the SSD is expected to be further increased by tuning some other parameters such as the trench width, the dielectric material that fills the trenches or by proposing channel geometries other than the L-shape.[29]

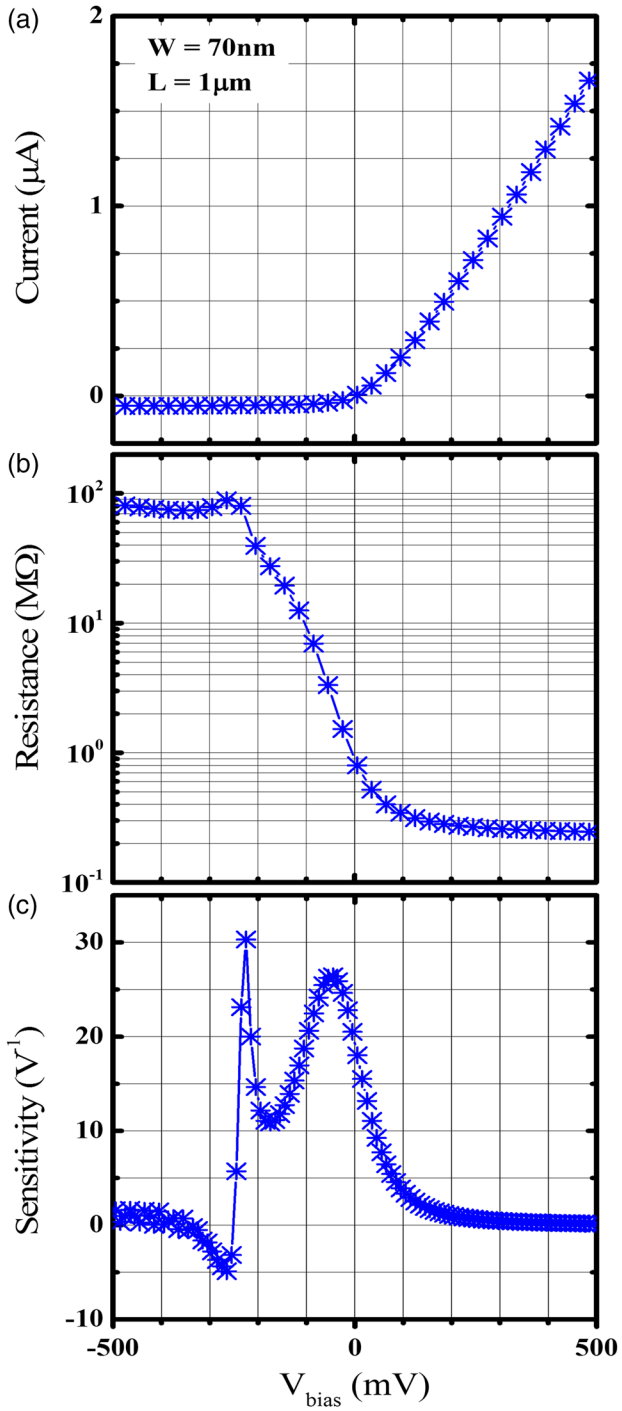

Fig. 3 (a) Current–voltage characteristic curve, (b) differential resistance, and (c) sensitivity values for the optimized L-shaped self-switching nanochannel with $W = 70$ nm and $L = 1$ μm.

3 Rectennas Based on Self-switching Diodes

We analyze the SSDs coupling to square- and Archimedean-spiral antennas shown in Fig. 4 due to their ideal frequency-independent behavior, which is of interest for energy harvesting applications. We consider the case of gold-made antennas (with refractive index, $n^* = 300 + 3j^*1000$) lying on the surface of a semi-infinite SiO_2 substrate ($n = 2$).[30,31] The antennas are tuned to resonate at wavelengths from 1.5 mm to 150 μm (200 GHz to 2 THz) with a right-hand circular polarization.

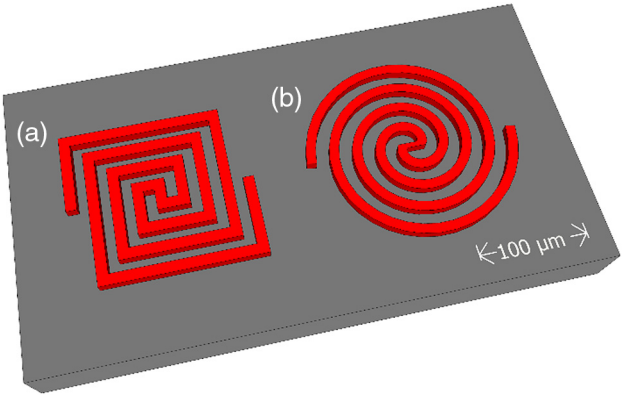

Fig. 4 Schematic representation of the proposed (a) square-spiral and (b) Archimedean-spiral broadband terahertz antennas used in this study.

The impedance of the antennas, Z_A, (Fig. 5) is evaluated by numerical simulations. In the analysis, the devices were excited with monochromatic plane waves with an irradiance of 1 W/cm^2,[32] incoming from a precisely tuned terahertz laser and through the simulations, the electric **E** and magnetic **H** field distributions were found. From these results, the antenna parameters were evaluated. For instance, Z_A is obtained by using the relationship

$$Z_A = \frac{V_{OC}}{I_{SC}}, \tag{2}$$

where V_{OC} is the voltage generated by the antennas at its open terminals[33] and I_{SC} is the current through the antennas when its terminals are short-circuited.[33] V_{OC} is obtained by evaluating the line integral of **E** along the circuit defined from one terminal to the other when nothing is connected to the antenna. The I_{SC} is obtained through the Ampere's law, integrating **H** along a closed-loop around one terminal, when terminals are short-circuited. Once the terahertz rectennas have been designed we introduce a simplified method to evaluate, from a theoretical perspective, the conversion efficiency of the devices.

When antennas operate at resonance they can be described by the equivalent circuit shown in Fig. 6.[26,33] An antenna behaves as a voltage source equal to V_{OC} with an internal real impedance

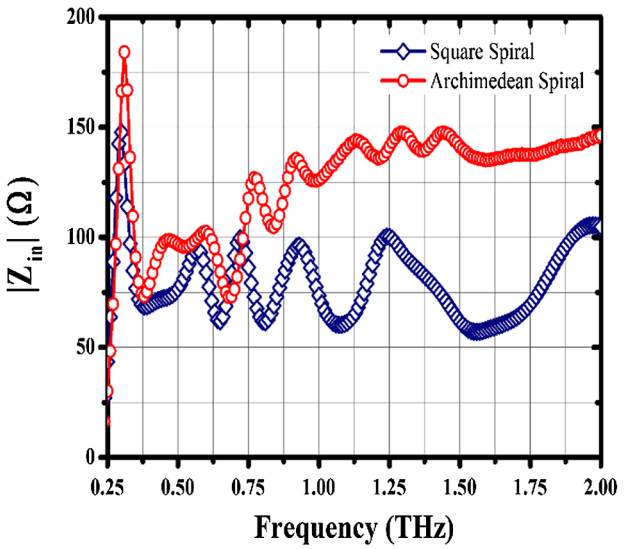

Fig. 5 Input impedance Z_{in} obtained by the simulation process as a function of frequency for the square- and Archimedean-spiral antennas.

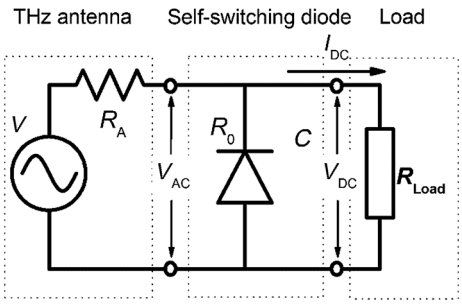

Fig. 6 Equivalent circuit model for an antenna coupled to a rectifying diode.

of value R_A.[26,33] In receive mode, V_{OC} is the voltage generated by the resonant antenna at its open terminals when nothing is connected. When a diode is coupled to the antenna feed gap, the antenna generates an AC voltage, V_{AC}, across the diode whose magnitude is given by

$$V_{AC} = \frac{V_{OC} \cdot Z_0}{(Z_0 + Z_A)}. \tag{3}$$

The V_{AC} across the diode in turn generates a rectified voltage, V_{DC}, according to Eq. (1). The DC power, P_{DC}, associated with the rectified voltage is given by

$$P_{DC} = \frac{V_{DC}^2}{R_0}. \tag{4}$$

On the other hand, the power, P, received by the antenna at the input port can be evaluated by using the relationship

$$P = P_{rad} + P_{loss}, \tag{5}$$

where, P_{rad} and P_{loss} are the power reemitted by the antenna and the power dissipated by the ohmic losses, respectively. Thus, the percentage conversion efficiency, η_e (%), of the antenna-coupled diode can be evaluated by the ratio of the DC power generated by the diode to the optical power received by the antennas as

$$\eta_e(\%) = \frac{P_{DC}}{P} \times 100. \tag{6}$$

We use the former relationships to study the case of the SSDs taking into account several simplifying assumptions. We consider that the DC transport properties of the diodes do not change with the frequency, at least not in the considered spectral range, which covers the frequency band from 200 GHz to 2 THz. The numerical simulations performed here are just a DC numerical analysis, since an AC analysis was not performed. This assumption is somehow justified by taking into account that the value of the cut-offs frequencies reported for high-mobility structures is around 5 THz.[16]

4 Rectennas Frequency Response

In Figs. 7(a) and 7(b), we have plotted the voltage and the DC electrical power generated from the incoming terahertz radiation as a function of frequency in the range from 0.2 to 2 THz (1.5 mm to 150 μm). These designs exhibit a full width at half-maximum parameter of more than 1.8 THz, a parameter that can be enhanced by increasing the number of turns contained by the spirals.

The DC power generated by the Archimedean spiral is larger than the power generated by the square spiral at high frequencies (above of 1.37 THz). The maximum peaks of power reach values around 1.8 and 0.6 μW, respectively. This fact is due to the considerable difference in their impedances in such a frequency regime (Fig. 5). The impedance of the Archimedean

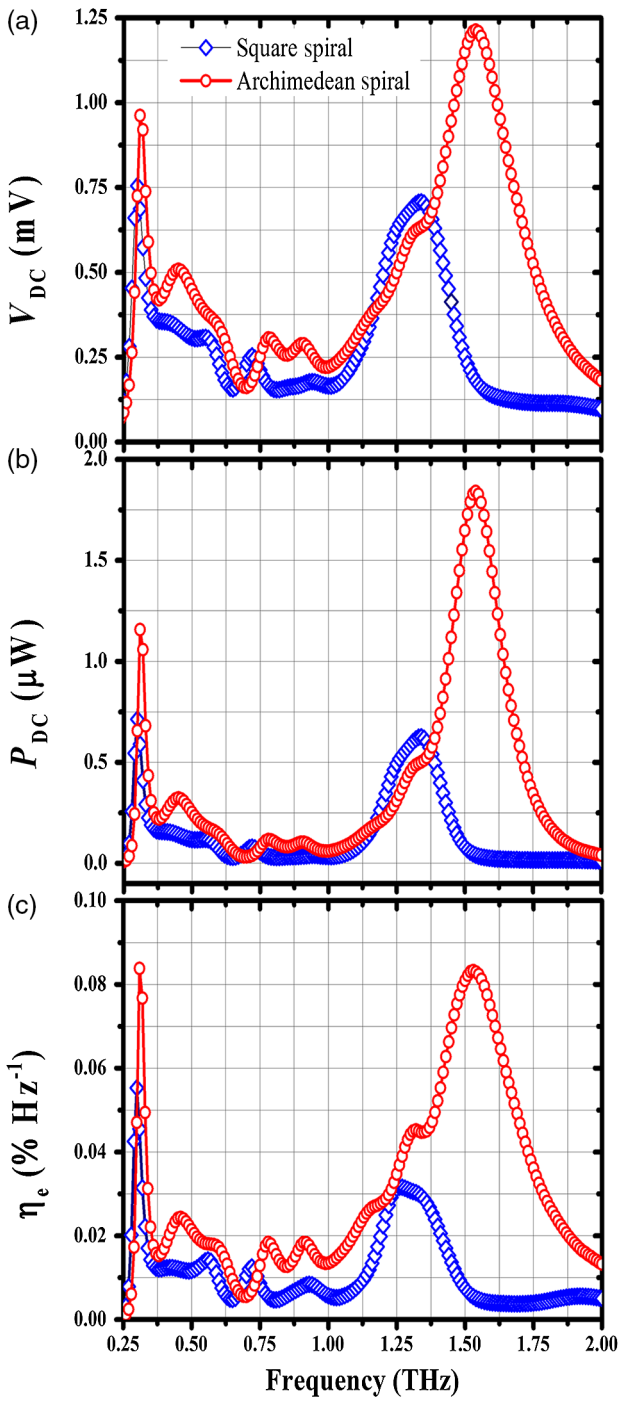

Fig. 7 Performance of the broadband rectennas to harvest the optical energy of a terahertz source (1 W/cm^2): (a) rectified voltage, (b) DC electrical power, and (c) optical-to-electrical conversion efficiency.

spiral is larger than the impedance of the square spiral by a factor of two for frequencies higher than 0.75 THz. A higher antenna impedance means a better electrical coupling between the antennas and the diode (due to the high R_0 of the SSD) and more efficient transfer of energy between both elements.

The conversion efficiency of the rectennas is shown in Fig. 7(c) as a function of frequency. Considering the specific application of harvesting the energy of terahertz radiation in the frequency band from 0.2 to 2 THz, the total efficiency η_{tot} can be calculated by using the relationship[5]

$$\eta_{\text{tot}} = \frac{\int_{0.2\ \text{THz}}^{2\ \text{THz}} S(f) \cdot \eta_{\text{e}}(f) \cdot \mathrm{d}f}{\int_{0.2\ \text{THz}}^{2\ \text{THz}} S(f) \mathrm{d}f}, \tag{7}$$

where $\eta_{\text{e}}(f)$ is the conversion efficiency of the rectennas as a function of the frequency and $S(f)$ is the irradiance of the terahertz source (for simplicity, 1 W/cm^2 at each single frequency). The total efficiencies of both types of devices are found to be ~0.032% and 0.013%, for Archimedean and square spiral, in that order. It is observed that by using L-shaped SSDs as fast rectifiers instead of metal–insulator–metal nanometer diodes (such as $\text{Al/Al}_2\text{O}_3\text{/Pt}$ diodes),[34] the efficiency of the rectennas can be increased by a factor of 10^6. Rectennas based on SSDs are more efficient than those based on MIM barriers due to their current–voltage characteristic curves, which are more asymmetrical.

On the other hand, the relatively low efficiencies ($\sim 10^{-2}\%$) are mainly attributed to the mismatch impedance between the rectifier and the antenna. This fact can be verified by evaluating the coefficient of reflection between both elements, and is defined as

$$\Gamma = \frac{R_0 - Z_{\text{in}}}{R_0 + Z_{\text{in}}}, \tag{8}$$

which exhibits average values around 99.96% and 99.8% for the Archimedean and square spiral, respectively. Reflection coefficient values indicate that only 0.04% and 0.02% of the optical energy is transmitted from the spirals to the self-switching nanodiodes and the rest of the optical power is returned to the spirals. By comparing transmitted power to nanodiodes (0.04% and 0.02% for Archimedean and square spiral, respectively) and the overall efficiency of the rectennas (~0.032% and 0.013% for Archimedean and square spiral, respectively), it can be seen that the efficiency of the rectifiers is high.

5 Conclusion

In summary, we have determined the efficiency of experimentally realizable rectennas based on different types of spiral antennas and evaluated their performance as terahertz energy harvesters. We focused on Archimedean and square spiral antennas in which optimized L-shaped self-switching nanodiodes were coupled as fast rectifiers. Simulations show that the proposed rectennas are able to reach overall efficiencies of ~0.032% and 0.013%, respectively. A rough estimation of the reflection coefficient reveals that most of the optical power is reflected from the diode to the spirals due to a remarkable difference in their electrical impedance. Among the advantages, these harvesters represent a suitable alternative to the rectennas based on MIM tunnel barriers, which exhibit very low efficiencies. It is worth mentioning that the presence of the SSDs reduces the technological process required for the rectennas' manufacture, implying only one step of high-resolution lithography. However, to produce terahertz rectennas useful for energy harvesting applications, an efficient strategy to better match the impedance of the spiral antennas and the self-switching nanodiodes should be incorporated.

Acknowledgments

The authors acknowledge the financial support from CEMIE-SOL 22, FRC-UASLP, and CONACYT-Mexico through grants: INFR-2015-01-255489, CB 2015-257358, PNCPN2014-01-248071, and SNI-CVU40859.

References

1. M. Bareiss et al., "Rectennas revisited," *IEEE Trans. Nanotechnol.* **12**(6), 1144–1150 (2013).
2. L. Olmon and M. B. Raschke, "Antenna-load interactions at optical frequencies: impedance matching to quantum systems," *Nanotechnology* **23**(44), 444001 (2012).
3. L. Mescia and A. Massaro, "New trends in energy harvesting from earth long-wave infrared emission," *Adv. Mater. Sci. Eng.* **2014**, 1–40 (2014).

4. Z. Ma and G. A. E. Vandenbosch, "Optimal solar energy harvesting efficiency of nano-rectenna systems," *Sol. Energy* **88**, 163–174 (2013).
5. G. A. E. Vandenbosch and Z. Ma, "Upper bounds for the solar energy harvesting efficiency of nano-antennas," *Nano Energy* **1**(3), 494–502 (2012).
6. S. J. Byrnes, R. Blanchard, and F. Capasso, "Harvesting renewable energy from Earth's mid-infrared emissions," *Proc. Natl. Acad. Sci. U. S. A.* **111**(11), 3927–3932 (2014).
7. M. Gallo et al., "Design of optical antenna for solar energy collection," *Energy* **39**(1), 27–32 (2012).
8. G. Consolmagno and M. W. Schaefer, *Worlds Apart: A Textbook in Planetary Sciences*, Benjamin Cummings, United States (1994).
9. N. Shinohara, "Rectennas for microwave power transmission," *IEICE Electron. Express* **10**(21), 20132009 (2013).
10. J. Bean, A. Weeks, and G. D. Boreman, "Performance optimization of antenna-coupled Al/AlOx/Pt tunnel diode infrared detectors," *IEEE J. Quantum Electron.* **47**(1), 126–135 (2011).
11. N. Alimardani and J. F. Conley, "Step tunneling enhanced asymmetry in asymmetric electrode metal-insulator-insulator-metal tunnel diodes," *Appl. Phys. Lett.* **102**(14), 143501 (2013).
12. C. Fumeaux, J. Alda, and G. D. Boreman, "Lithographic antennas at visible frequencies," *Opt. Lett.* **24**(22), 1629–1631 (1999).
13. S. Grover and G. Moddel, "Applicability of metal/insulator/metal (MIM) diodes to solar rectennas," *IEEE J. Photovolt.* **1**(1), 78–83 (2011).
14. G. Moddel, "Optical rectennas: nanotubes circumvent trade-offs," *Nat. Nanotechnol.* **10**, 1009–1010 (2015).
15. R. Hussin, Y. Chena, and Y. Luob, "Metal-semiconductor-metal heterojunction diodes consisting of a thin layer of crystal silicon," *Appl. Phys. Lett.* **102**, 093507 (2013).
16. A. M. Song et al., "Unidirectional electron flow in a nanometer-scale semiconductor channel: a self-switching device," *Appl. Phys. Lett.* **83**(9), 1881–1883 (2003).
17. C. Balocco et al., "Microwave detection at 110 GHz by nanowires with broken symmetry," *Nano Lett.* **5**(7), 1423–1427 (2005).
18. C. Balocco et al., "Room-temperature operation of a unipolar nanodiode at terahertz frequencies," *Appl. Phys. Lett.* **98**(22), 223501 (2011).
19. J. Mateos et al., "Operation and high-frequency performance of nanoscale unipolar rectifying diodes," *Appl. Phys. Lett.* **86**(21), 212103 (2005).
20. A. Westlund et al., "Terahertz detection in zero-bias InAs self-switching diodes at room temperature," *Appl. Phys. Lett.* **103**(13), 133504 (2013).
21. Y. Pan et al., "Micro rectennas: Brownian ratchets for thermal-energy harvesting," *Appl. Phys. Lett.* **105**(25), 253901 (2014).
22. A. M. Song et al., "Diode-like characteristics of nanometer-scale semiconductor channels with a broken symmetry," *Phys. E.* **21**(4), 1116–1120 (2004).
23. G. Farhi et al., "The impact of etched trenches geometry and dielectric material on the electrical behavior of silicon-on-insulator self-switching diodes," *Nanotechnology* **22**(43), 435203 (2011).
24. K. Y. Xu, G. Wang, and A. M. Song, "Electron transport in self-switching nano-diodes," *J. Comput. Electron.* **6**(1), 59–62 (2007).
25. A. K. Baraskar et al., "Ultralow resistance, nonalloyed Ohmic contacts to n-InGaAs," *J. Vac. Sci. Technol. B* **27**, 2036–2039 (2009).
26. A. Sanchez et al., "The MOM tunneling diode: theoretical estimate of its performance at microwave and infrared frequencies," *J. Appl. Phys.* **49**(10), 5270–5277 (1978).
27. M. N. Gadalla, M. Abdel-Rahman, and A. Shamim, "Design, optimization and fabrication of a 28.3 THz nano-rectenna for infrared detection and rectification," *Sci. Rep.* **4**, 4270 (2014).
28. M. Dagenais et al., "Solar spectrum rectification using nano-antennas and tunneling diodes," *Proc. SPIE* **7605**, 76050E (2010).
29. I. E. Cortes-Mestizo et al., "Study of InAlAs/InGaAs self-switching diodes for energy harvesting applications," *Jpn. J. Appl. Phys.* **55**, 014304 (2016).

30. H. Yasuda and I. Hosako, "Measurement of terahertz refractive index of metal with terahertz time-domain spectroscopy," *Jpn. J. Appl. Phys.* **47**, 1632–1634 (2008).
31. I. Hosako, "Optical thin film technology used in the terahertz frequency," *J. Nat. Inst. Inf. Commun. Technol.* **51**(1), 87–94 (2004).
32. B. Zhang et al., "Conjugated polymer-based broadband terahertz wave modulator," *Opt. Lett.* **39**(21), 6110–6113 (2014).
33. C. A. Balanis, *Antenna Theory: Analysis and Design*, John Wiley & Sons, Inc., New York (1996).
34. E. Briones, J. Alda, and F. J. González, "Conversion efficiency of broad-band rectennas for solar energy harvesting applications," *Opt. Express* **21**(S3), A412–A418 (2013).

Edgar Briones received his BS degree in theoretical physics from the Autonomous University of San Luis Potosi, San Luis Potosi, Mexico, in 2003 and his MS degree in sciences from the same institution, in 2006. He received his PhD in physics from the Laboratoire de Photonique et de Nanostructures, Université Paris XI, Orsay, France, in 2010. Currently, he is an associate researcher at the Jesuit University of Guadalajara, ITESO AC.

Irving E. Cortes-Mestizo obtained his BS degree in electronic and communications engineering in 2012 and his MSc degree in micro-and nanosystems in 2014 from Veracruzana University, Veracruz, Mexico. Currently, he is a PhD student at the Autonomous University of San Luis Potosi, San Luis Potosi, Mexico. His research interests are optical characterization, numerical analysis, and applications of semiconductor nanostructures.

Victor H. Mendez-Garcia received his PhD in physics from CINVESTAV-Mexico in 1999. He joined UASLP in 2000. Since, 2009 he has headed the Nanostructures Laboratory at CIACYT-UASLP, the largest MBE lab in Latin America. His research on low dimensional systems covers architecture of nanostructures on high index substrates for optoelectronics, photovoltaic devices, thermal energy harvesting, and THz technologies.

Biographies for the other authors are not available.